

A correlation for predicting the critical heat flux condition with twisted-tape swirl generators

MICHAEL K. JENSEN

Department of Mechanical Engineering, University of Wisconsin—Milwaukee, Milwaukee, WI 53201, U.S.A.

(Received 17 November 1983 and in revised form 27 January 1984)

NOMENCLATURE

a/g	nondimensional acceleration
Bo	boiling number, q''_{cr}/GH_{fg}
D	tube diameter [m]
g	gravitational acceleration [m s^{-2}]
G	mass velocity [$\text{kg m}^{-2} \text{s}^{-1}$]
ΔH_i	enthalpy of inlet subcooling or quality [J kg^{-1}]
H_{fg}	enthalpy of evaporation [J kg^{-1}]
K	parameter for nonsaturated inlet conditions
L	length [m]
p	pressure [N m^{-2}]
q''	heat flux [W m^{-2}]
V	axial velocity [m s^{-1}]
x	quality
y	tape-twist ratio (length for 180° twist/inside tube diameter).

Greek symbol

ρ	density [kg m^{-3}].
--------	---------------------------------

Subscripts

cr	critical
g	vapor
l	liquid
s	saturated
tt	twisted tape.

INTRODUCTION

Twisted-tape swirl generators have been studied extensively for various two-phase flow conditions [1, 2], with the main emphasis being placed on determining the effect of twisted-tape inserts on the suppression of the critical heat flux (CHF) condition. Both subcooled and quality regime CHF data have been obtained with several fluids, fluid conditions and tape geometries [3–13]. From the quality region studies, it is evident that the CHF can be raised significantly compared to a straight empty tube at the same local flow conditions and that

the total power input to the tube can be about 1.2–2 times that of the smooth tube. This enhancement depends on the tape-twist ratio y (length for 180° twist/inside tube diameter), pressure level, quality, and mass velocity. Whalley [14] has shown that in the two-phase region because of centrifugal forces, the liquid film flow rate is increased with twisted tapes with the result being that the onset of the CHF condition is delayed. However, no correlations have been presented in the literature with which general predictions could be made for the quality region CHF with twisted-tape inserts. Thus, the present paper reports a new correlation with which predictions can be made for the CHF condition in the quality region over a wide range of flow conditions.

ANALYSIS

From the literature, many papers were found which addressed the CHF condition in the quality regime. However, only eight contained enough information to analyze the data in detail [3–10]. These studies are listed in Table 1 with the geometry and flow conditions covered. As can be seen from this table, a very wide range of conditions have been covered in these studies. Of these papers, only four had straight empty tube reference data [3, 6–8].

Reference data or predictions for the CHF in axial flow were required to evaluate and correlate the effect of the twisted-tape inserts. Four correlations (Thompson and Macbeth [15], Biasi *et al.* [16], Groeneveld and Rousseau [17], and Katto [18–20]) from the literature were tested against the axial flow reference data in refs. [3, 6–8]. Both the local CHF and the overall power approaches were tried. Of these, the correlations suggested by Katto [18–20] predicted the axial flow CHF data the best when the inlet fluid conditions for the various data points were used with the tube geometry. Thus, the overall power input to the tube was predicted and not the CHF at the local fluid conditions (local quality, mass velocity, and pressure). Using the CHF correlations developed by Katto [18–20], the CHF for inlet flow conditions different than

Table 1. Ranges of conditions for swirl flow data

Ref.	Fluid	L (mm)	D (mm)	y	P (kN m^{-2})	G ($\text{kg m}^{-2} \text{s}^{-1}$)	x_{cr}	No. of data points
3	water	4877	10.16	15.00	6900	1260–4600	0.33–0.88	27
4	water	2000	10.00	3.00	5070	760–1040	0.81–0.88	37
5	water	457	8.00	2.50; 5.0	13 800	670–2700	0.01–0.53	44
6	R-22	1539	10.16	16.25	1310	510–1280	0.52–0.84	11
7	water	1016	11.43	5.55; 34.50	7000	390–1150	0.74–0.95	9
8	water	1064	20.00	3.00; 6.00	101	120–510	0.29–0.99	6
9	water	280	7.00	2.32; 5.71	7000; 10 100	2300–3530	0.01–0.23	71
10	water	800	10.00	3.00	6900	4480–5840	0.15–0.19	2

saturation was calculated with

$$Bo = Bo_s(1 + K\Delta H_v/H_{fg}) \tag{1}$$

where Bo_s is the boiling number calculated for saturated inlet conditions and K is a parameter to account for nonsaturated conditions at the inlet. The parameters Bo_s and K have different correlations depending on the CHF regime as identified by Katto. These correlations are listed in refs. [18–20]. In addition, various guidelines for the use of the correlations, particularly when the inlet condition is not a saturated fluid, are given.

A total of 66 axial flow data points were tabulated. (The axial and swirl flow data from Staub's [6] Tables I and II show a discrepancy between the enthalpy gain of the fluid and the power dissipation in the tube. According to Katto [21] the correct data should be based on the enthalpy gain of the fluid. This correction was made to Staub's data so that this data could be used.) The majority of the axial flow data fell in the H regime, with some in the HP regime. Comparing these data to the predictions, the average ratio of the predicted data to the experimental data was 0.962 and the average deviation between the experimental data and the predicted values was $\pm 10.4\%$. Because of this good agreement between the reference data and the predictions, Katto's correlations were used as the reference against which all the twisted-tape data were compared.

As noted previously not all investigations provided enough information to analyze the twisted-tape data in detail. The data which were used were examined closely to eliminate those data which did not satisfy the inlet fluid conditions needed to use Katto's correlations for predicting the axial flow CHF when using the inlet conditions from the twisted-tape data. (Only data with a critical quality greater than 0.01 were used.) In addition, Moeck *et al.* [7] found a decrease in the twisted-tape CHF below that of the axial flow CHF if the amount of liquid in the flow, $G(1 - x)$, was less than approximately $80 \text{ kg m}^{-2} \text{ s}^{-1}$. This was attributed to the tape capturing some of the liquid in the flow. These data were rejected, as were data from other investigations which met this condition. The resulting 207 data points were then evaluated.

The main effect of the twisted tapes is to impart to the flowing fluid a centrifugal acceleration. Liquid droplets entrained in the vapor flow are affected more than the vapor and are centrifuged to the walls of the tube. With a change in the difference between the liquid and vapor densities, one would expect the effect of the centrifugal acceleration to change. The nondimensional centrifugal acceleration can be

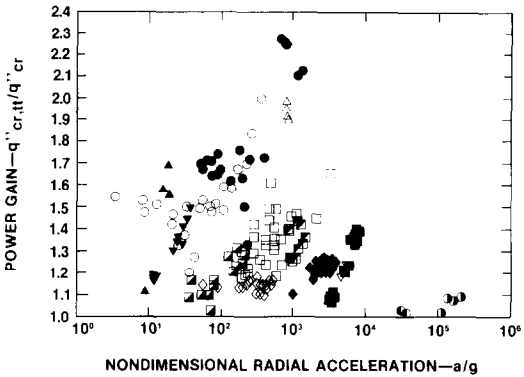


FIG. 1. Nondimensionalized CHF for twisted-tape swirl generators for a variety of flow conditions and geometries.

calculated by

$$(a/g) = (2/Dg)(V\pi/2y)^2 \tag{2}$$

where the axial velocity $V = G/\rho$ is evaluated using the homogeneous density. Thus, the radial acceleration increases with a tighter tape twist (smaller y), quality and mass velocity. The twisted-tape CHF (or critical power since all of these studies involved constant wall heat flux boundary conditions) was nondimensionalized by the CHF (or power) as calculated by Katto's correlations when using the same geometry and inlet fluid conditions as the twisted-tape data. As with the axial flow data, the majority of the data fell into the H regime, with some in the HP and N regimes. The nondimensional power ratio is plotted in Fig. 1 as a function of the nondimensional radial acceleration. The symbols used in Fig. 1 are identified in Table 2.

RESULTS

While there is considerable scatter in the data shown in Fig. 1, there does appear to be a consistent pattern in the data in relation to the acceleration and density ratios. There generally is a shift in the data corresponding to the varying density ratio level. With increasing pressure the data shift toward the left and tend to show an increased gain in power. At any one pressure level the data show an increasing CHF with

Table 2. Legend for Figs. 1 and 2

	Ref.*	ρ_l/ρ_g	y
□	3	20.7	15.00
■	4	30.6	3.00
○	5	7.5	2.50
●	5	7.5	5.00
▼	6	20.6	16.25
△	7	20.3	5.55
▲	7	20.3	34.50
◐	8	1605.4	3.00
◑	8	1605.4	6.00
◆	9	20.3	2.32
◼	9	12.4	2.32
◊	9	20.3	5.71
◻	9	12.4	5.71
▽	10	20.7	3.00

* Fluid used is water for all studies except in ref. [6] where the fluid is R-22.

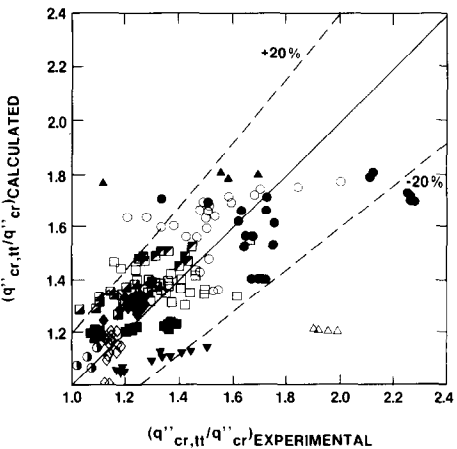


FIG. 2. Comparison between the experimental and calculated power gain with twisted tapes.

increasing acceleration. Note also the shift in the data with increasing tape-twist ratio. As y increases the data are shifted toward the left for any given pressure ratio. This is demonstrated most clearly for the density ratio of approximately 20.7.

To correlate the data, a nonlinear regression analysis was performed on the data. The resulting correlation

$$(q''_{cr,u}/q''_{cr}) = (4.597 + 0.09254y + 0.004154y^2)(\rho_l/\rho_g)^{-0.7012} + 0.09012 \ln(a/g) \quad (3)$$

predicted the data well with the average ratio of predicted data to experimental data of 1.015 and with an average deviation between the experimental data and the prediction of $\pm 10.2\%$. The scatter in the data is shown in Fig. 2; 81% of the data are predicted to within $\pm 15\%$ and 91% are predicted to within $\pm 20\%$. Note that to use this correlation an iterative solution is required. Any CHF ratio predicted to be less than unity should be set to unity.

CONCLUSIONS

The CHF condition for twisted-tape generated swirl flow has been examined. Data from many investigations covering a very wide range of flow conditions and geometries have been tabulated. By using Katto's axial flow correlations to nondimensionalize the CHF data from swirl flows, a nondimensional radial acceleration to characterize the centrifuging effect on entrained liquid droplets, and the liquid-to-vapor density ratio to describe the pressure level, the data were successfully correlated.

Acknowledgement—This research is based on work supported by the National Science Foundation under Grant No. MEA-8117226.

REFERENCES

1. A. E. Bergles, R. L. Webb, G. H. Junkhan and M. K. Jensen, Bibliography on augmentation of convective heat and mass transfer, Heat Transfer Laboratory Report HTL-19, ISU-ERI-AMES-79206, Iowa State University, Ames, Iowa, May (1979).
2. W. R. Gambill and R. D. Bundy, An evaluation of the present status of swirl-flow heat transfer, ASME Paper No. 62-HT-42 (1962).
3. B. Matzner, E. O. Moeck, J. E. Casterline and G. A. Wikhammer, Critical heat flux in long tubes at 1000 psi with and without swirl promoters, ASME Paper No. 65-WA/HT-30 (1965).
4. R. Brevi, M. Cumo, A. Palmieri and D. Pitimada, Forced convection heat transfer and burnout measurements with twisted-tapes, *Termotecnica*, **26**, 619–625 (1971).
5. R. Viskanta, Critical heat flux for water in swirling flow, *Nucl. Sci. Eng* **10**, 202–203 (1961).
6. F. W. Staub, Two-phase fluid modelling—the critical heat flux, *Nucl. Sci. Engng* **35**, 190–199 (1963).
7. E. V. Moeck, G. A. Wikhammer, I. P. L. MacDonald and J. G. Collier, Two methods of improving the dryout heat flux for high pressure steam/water flow, AECL Report No. 2109, December (1964).
8. A. Rosuel and G. Sourieux, Influence de Tourbillons Induits dans l'Eau Bouillante a la Pression Atmospherique sur les Flux de Calefaction, Rapport EURATOM No. 5, S.N.E.C.M.A., Division Atomique (1961).
9. D. Henkel, F. Mayinger, O. Schad and E. Weiss, Untersuchung der Kritischen Heizflaechenbelastung (Burnout) bei Seidendem Wasser, M.A.N. Report No. 09.02.07, July (1965).
10. A. Rosuel, G. Sourieux and J. Dolle, Ecoulements Giratoires dans l'Eau Bouillante, Rapport EURATOM No. 16, S.N.E.C.M.A., Division Atomique (1963).
11. W. R. Gambill, R. D. Bundy and R. W. Wansbrough, Heat transfer, burnout, and pressure drop for water in swirl flow through tubes with internal twisted-tapes. *Chem. Engng Prog. Symp. Ser.* **57**(32), 127–137 (1961).
12. L. Feinstein and R. C. Lundberg, Fluid friction and boiling heat transfer with water in vortex flow in tubes containing an internal twisted-tape, RADC-TRR-63-451, AD430889, June (1963).
13. W. R. Gambill and R. D. Bundy, High-flux heat transfer characteristics of pure ethylene glycol in axial and swirl flow, *A.I.Ch.E. J* **9**, 55–59 (1963).
14. P. B. Whalley, The effect of swirl flow on critical heat flux in annular two-phase flow, *Int. J. Multiphase Flow* **5**, 211–217 (1979).
15. B. Thompson and R. V. Macbeth, Boiling water heat transfer—burnout in uniformly heated round tubes: a compilation of world data with accurate correlations, AEEW-R356 (1964).
16. L. Biasi, G. C. Clerici *et al.*, Studies on burnout: Part 3, *Energia Nucl.* **14**(9), 530–536 (1967).
17. D. C. Groeneveld and J. C. Rousseau, CHF and post-CHF heat transfer: an assessment of prediction methods and recommendations for reactor safety codes, in *Advances in Two-phase Flow and Heat Transfer* (edited by S. Kakac and M. Ishii), pp. 203–237. Martinus Nijhoff, Boston (1983).
18. Y. Katto, A generalized correlation of critical heat flux for the forced convection boiling in vertical uniformly heated round tubes, *Int. J. Heat Mass Transfer* **21**, 1527–1542 (1978).
19. Y. Katto, An analysis of the effect of inlet subcooling on critical heat flux of forced convection boiling in vertical uniformly heated tubes, *Int. J. Heat Mass Transfer* **22**, 1567–1575 (1979).
20. Y. Katto, Critical heat flux of forced convection boiling in uniformly heated vertical tubes (correlation of CHF in HP-regime and determination of CHF-regime map), *Int. J. Heat Mass Transfer* **23**, 1573–1580 (1980).
21. Y. Katto, A generalized correlation of critical heat flux for the forced convection boiling in vertical uniformly heated round tubes—a supplementary report, *Int. J. Heat Mass Transfer* **22**, 783–794 (1979).